Published in final edited form as:

Cancer Res. 2017 March 15; 77(6): 1283–1295. doi:10.1158/0008-5472.CAN-15-3545.

Bone pain induced by multiple myeloma is reduced by targeting V-ATPase and ASIC3

Masahiro Hiasa[1], **Tatsuo Okui**[1], **Yohance M Allette**[2], **Matthew S Ripsch**[2], **Ge-Hong Sun-Wada**[3], **Hiroki Wakabayashi**[4], **G David Roodman**[1,5], **Fletcher A. White**[2], and **Toshiyuki Yoneda**[1]

[1]Division of Hematology and Oncology, Paul and Carole Stark Neurosciences Research Institute, Indiana University School of Medicine, Indianapolis, IN, USA

[2]Department of Anesthesia, Paul and Carole Stark Neurosciences Research Institute, Indiana University School of Medicine, Indianapolis, IN, USA

[3]Department of Biochemistry, Faculty of Pharmaceutical Sciences, Doshisha Women's College, Kyoto

[4]Department of Orthopaedic Surgery, Mie University Graduate School of Medicine, Mie, Japan

[5]The Rodebusch VA, Indianapolis, IN, USA

Abstract

Multiple myeloma (MM) patients experience severe bone pain (MMBP) that is undertreated and poorly understood. In this study, we studied MMBP in an intratibial mouse xenograft model which employs JJN3 human MM cells. In this model, mice develop MMBP associated in bone with increased sprouting of calcitonin gene-related peptide-positive (CGRP+) sensory nerves and in dorsal root ganglia (DRG) with upregulation of phosphorylated ERK1/2 (pERK1/2) and pCREB, two molecular indicators of neuron excitation. We found that JJN3 cells expressed a vacuolar proton pump (V-ATPase) that induced an acidic bone microenvironment. Inhibition of JJN3-colonized bone acidification by a single injection of the selective V-ATPase inhibitor, bafilomycin A1, decreased MMBP, CGRP+ SN sprouting, and pERK1/2 and pCREB expression in DRG. CGRP+ sensory nerves also expressed increased levels of the acid-sensing nociceptor ASIC3. Notably, a single injection of the selective ASIC3 antagonist APETx2 dramatically reduced MMBP in the model. Mechanistic investigations in primary DRG neurons co-cultured with JJN3 cells showed increased neurite outgrowth and excitation inhibited by bafilomycin A1 or APETx2. Further, combining APETx2 with bafilomycin A1 reduced MMBP to a greater extent than either agent alone. Lastly, combining bafilomycin A1 with the osteoclast inhibitor zoledronic acid was sufficient to ameliorate MMBP which was refractory to zoledronic acid. Overall, our results show that osteoclasts and MM cooperate to induce an acidic bone microenvironment that evokes MMBP as a result of the excitation of ASIC3-activated sensory neurons. Further, they present a

Corresponding author: Dr. Toshiyuki Yoneda, Division of Hematology and Oncology, Indiana University School of Medicine, Walther Hall, R3-C321D, 980 W Walnut St, Indianapolis, IN 46202, USA, Phone: 317-274-3530; Fax: 317-274-0396; toshyone@iu.edu.

G.D. Roodman is a consultant/advisory board member for Amgen. No potential conflicts of interest were disclosed by the other authors.

mechanistic rationale for targeting ASIC3 on neurons along with the MM-induced acidic bone microenvironment as a strategy to relieve MMBP in patients.

Keywords

Osteoclastic bone destruction; bisphosphonates; acidic microenvironment; sensory neurons; nociceptors

Introduction

Multiple myeloma (MM) is a malignant plasma cell disorder accounting for approximately 10% of all hematologic cancers (1). Seventy percent of MM patients present with severe bone pain associated with osteolytic bone lesions that result from increased osteoclastic bone resorption and reduced osteoblastic bone formation (2). Bone pain contributes to increased mortality and morbidity (3). The degree of bone pain in MM is often greater than pain experienced with solid tumors (4–6) and bone pain is the most common presenting complaint of MM patients (7). Control of bone pain is thus a major goal in the management of MM patients. Despite this, the pathophysiology of bone pain associated with MM (MMBP) is poorly understood, and MMBP is frequently inadequately treated (3).

Bone is densely innervated by sensory neurons (SNs), especially the calcitonin gene-related peptide-positive ($CGRP^+$) SN (8–12), which show pathological sprouting in the presence of tumors (13,14). Osteoclasts (OCLs) are also increased in cancer-colonized bone and actively secrete protons (H^+) to destroy mineralized bone via the plasma membrane a3 isoform vacuolar-H^+-ATPase (a3V-ATPase) localized in the ruffled borders (15), creating an acidic microenvironment (pH range = 4.0–6.0) (16,17). H^+ are a well-known potent pain-inducing mediator (18,19), suggesting that the acidic microenvironment created by increased H^+ release from bone-resorbing OCLs via the a3V-ATPase activates pH-sensitive SNs to elicit bone pain. Consistent with this notion, specific inhibitors of osteoclastic bone resorption, including bisphosphonates (BPs) and denosumab (Dmab), significantly reduce bone pain in patients with MM (2,20) and bone metastases of solid cancers (21–23), indicating that OCL bone resorption contributes to activation of nociceptive SNs in bone to induce bone pain.

However, BP or Dmab treatment does not prevent the progression of bone pain in bone metastasis at advanced stages in patients with solid tumors (22,23), suggesting that tumor cells also contribute to bone pain. Solid tumor cells release increased levels of H^+ via various types of plasma membrane pH regulators, thereby inducing an acidic extracellular microenvironment (pH range = 6.5–7.0) (24,25) that can also excite pH-sensitive nociceptive SNs innervating bone to evoke bone pain. Similarly, it has been clinically well-recognized that MMBP in patients at advanced stages is unresponsive to BPs or Dmab. Thus, MM cells may also contribute to induce MMBP through creation of acidic extracellular microenvironment via plasma membrane pH regulators as do solid tumors.

A subpopulation of peripheral nerve fibers, termed nociceptors (18), recognize and transduce local nociceptive stimuli into electrochemical signals. The nociceptors in turn transmit these noxious signals to the central nervous system (CNS) and brain via the dorsal

root ganglion (DRG), which is the cell body of primary afferent SN fibers innervating peripheral tissues and serves as the gateway for peripheral noxious signals to the CNS (26). The specific acid-sensing nociceptors related to acid-induced bone pain are the transient receptor potential channel-vanilloid subfamily member 1 (TRPV1) and the acid-sensing ion channel 3 (ASIC3) (18). TRPV1 is activated by pH values < 6.0 (27), equivalent to the pH under the OCL ruffled border (15–17). Previous studies reported that TRPV1 plays a critical role in cancer-associated bone pain (28,29). In contrast, little is known about contributions of ASIC3 to bone pain, despite that ASIC3 senses milder pH between 6.5 and 7.0 (30), equivalent to the pH of the bone microenvironment of cancer-involved bone (24,25).

In this study, we show that H^+ released via V-ATPase by bone-resorbing OCLs and JJN3 MM cells create an acidic bone microenvironment that excites SNs innervating bone via activation of ASIC3 to induce MMBP. Further, blocking the generation of the acidic bone microenvironment and the activation of ASIC3 on SNs significantly reduced MMBP and could be a mechanism-based therapeutic approach for MMBP.

Materials and Methods

Reagents

The sources for the reagents were as follows. APETx2 and SB366791 (Tocris); zoledronic acid monohydrate (Sigma); rabbit monoclonal antibodies to, ERK1/2, CREB, pERK1/2, pCREB, HRP-conjugated horse anti-mouse IgG and goat anti-rabbit IgG antibody (Cell Signaling); bafilomycin A1, rabbit polyclonal antibodies to ASIC3, TRPV1, the goat polyclonal antibody against CGRP, and HRP-conjugated mouse monoclonal antibody against β-actin (Abcam); Alexa fluor 488-conjugated donkey anti-rabbit IgG and donkey anti-chicken IgY, and rhodamine red-X (RRX)-conjugated donkey anti-goat IgG antibody (Jackson); rhodamine phalloidin (Life Technologies); and rabbit polyclonal antibodies to RANKL, IL-6, mouse monoclonal antibody to MIP-1α, and HRP-conjugated goat anti-chicken antibody (Santa Cruz).

Cell culture

The JJN3 human MM cell line was provided by Dr. Giuliani (31). JJN3, H929 and U266 MM cell lines and primary $CD138^+$ MM cells and $CD138^-$ cells (isolated from bone marrow aspirates of MM patients using MACS MicroBead) were cultured in RPMI1640 medium with 5% FBS, 100 units/ml penicillin and 100 mg/ml streptomycin. The mouse osteocytic MLO-A5 and MLO-Y4 (Dr. Bellido), mouse osteoblastic MC3T3-E1, and F11 SN, human breast cancer (BC) MCF-7 and MDA-MB-231 cells were cultured in α-MEM (Gibco) with 10% FBS, 100units/ml penicillin and 100mg/ml streptomycin. Primary rat DRG SN (1° N) cells (Lonza) were cultured in Primary Neuron Growth Medium (Lonza) with 2% FBS. All cell lines were analyzed and authenticated by targeted genomic and RNA sequencing. All procedures involving patients were performed with written informed consent according to the Declaration of Helsinki and under a protocol approved by the Indiana University (IU) Institutional Review Board.

Animal model of MM

All animal studies were approved by the IACUC at IU School of Medicine. JJN3 cells (5×10^5) or PBS (sham) were injected into the right tibia marrow of female C57BL/6 SCID mice (4–6 week-old) under anesthesia (32).

Behavioral pain tests

Mechanical allodynia and thermal hyperalgesia were evaluated by von Frey and plantar tests using the Dynamic Plantar Aesthesiometer and Plantar Test Instrument (Ugo Basile), respectively (33,34). These tests are widely used for bone pain assessment in rodents (35). Tests were performed prior to MM cell injection to determine baseline behaviors and every 5 days following cell injection. Throughout the experiment, behavioral tests were performed under blind conditions by a single researcher. JJN3 cell injections were performed by a researcher blinded to the experiment. The investigator performing the behavioral tests was blinded as to the experimental condition of the animals.

Acridine orange accumulation

Acridine orange (Molecular Probes), which selectively deposits and fluoresces in acidic environments (36), was injected (1.0 mg/kg) into mice via the tail vein 2h prior to sacrifice. Tibiae were excised and acridine orange fluorescence detected using an EVOS fluorescence microscope (Advanced Microscopy).

Tartrate-resistant acid phosphatase (TRAP) staining

Bone sections were stained for TRAP activity using a TRACP & ALP double-stain Kit (Takara Bio) (32) and analyzed using Magnafire 4.1 software (Optronics) with the IX70 microscope (Olympus).

C-terminal telopeptides of type I collagen (CTx) measurement

Sera were collected from mice at indicated time, and CTx was measured by RatLaps™ (CTX-I) EIA kit (Immunodiagnosticsystems) according to manufacturer's instruction.

Extracellular pH (pH_e) measurement

Cells (10^5/96-well) were cultured for 48h in the presence of adriamycin (30nM) to prevent cell proliferation and pH_e was measured by FiveEasy pH meter (Metter Toled) immediately after removal from the CO_2 incubator.

Knockdown of a3V-ATPase in JJN3 cells

JJN3 cells were infected with 20μL of control (sc-108080) or TCIRG1 (sc-96928-V) shRNA lentiviral particles (Santa Cruz) in the presence of 5 μg/ml polybrene. One day later, cells were cultured in RPMI1640 plus 5% FBS for 7 days in the presence of 2 μg/ml puromycin (Gibco) to select cells stably expressing the shRNAs.

Neurite outgrowth determination

1° N cells (1×10^3/6-well) were co-cultured with JJN3 cells (5×10^3) or alone for 120h. Neurite outgrowth was visualized by staining the cultures with calcein AM (Life

technologies) and the length of neurites was quantified with a fluorescent microscope using Neuron J (37).

Imaging of intracellular Ca^{2+} influx

1° N or F11 SN cells were seeded in FluoroDish (World Precision) and loaded with fura-2 AM (3μM, Molecular Probes) for 25 min (38). Intracellular calcium was measured by digital video microfluorometry, using an intensified CCD camera coupled to a microscope and MetaFluor software (Molecular Devices). Cells were illuminated, and the excitation wavelengths for fura-2 (340/380 nm) were selected by a filter changer. Inhibitors were added directly into the bathing solution 2h before stimulation with 0.1N hydrochloric acid (HCl).

Immunoblotting

Cells or tissues were lysed in lysis buffer (Invitrogen), electrophoresed on a 10% SDS-PAGE, and blotted onto PVDF membranes (Biorad) (32). After blocking, the membranes were incubated with primary antibodies overnight at 4 °C, and then with HRP-conjugated secondary antibodies for 1h. Protein bands were visualized with a SuperSignal West Pico Chemiluminescent Substrate (Thermo Fisher).

Immunohistochemistry (IHC)

Bones were fixed, embedded in OCT compound and sectioned at 30μm thickness using a cryostat. After blocking, sections were incubated with the primary antibodies overnight at 4°C, and secondary antibodies for 60 min, mounted with coverslips in VECTASHIELD anti-fade mounting medium (Vector) and observed under the Leica TCS SP8 confocal laser scanning microscope.

For TRAP and CGRP double-staining, sections were first stained with TRAP and incubated with anti-CGRP antibody (1/200) overnight at 4°C, and then with HRP-conjugated secondary antibodies and diaminobenzidine substrate (Vector).

Immunocytochemistry (ICC)

JJN3 cells (1×10^3/96-well) were fixed with 10% neutral-buffered formalin, incubated with 3% BSA-PBS blocking solution, and then with a3V-ATPase antibody (1/200) (39) at 4°C overnight, followed by Alexa Fluor® 594 anti-chicken secondary antibody (1/1,000) and Alexa Fluor® 488 Phalloidin (1/2,000) were then added. Nuclei were counter-stained with DAPI.

Statistical analysis

Data are presented as the mean ± SEM. Statistical differences were determined by parametric or nonparametric tests as indicated.

Results

Animal model of MMBP

Mice intratibially injected with JJN3 cells developed characteristic osteolytic lesions on X-ray (Figure 1A) and μCT (Figure 1B). These lesions showed aggressive proliferation of JJN3

cells in bone marrow (Figure 1C) with increased $TRAP^+$ OCL bone resorption (Figure 1D, 1E) and elevated serum CTx (Figure 1F). We found that JJN3 cells produced osteoclastogenic cytokines including RANKL, IL-6 and MIP-1α (Figure 1G). Interestingly, MDA-MB-231 human breast cancer cells (25), used as a representative aggressive solid cancer cells that develop osteolytic bone lesions to compare with MM cells, showed undetectable production of MIP-1α. PBS-injected sham mice exhibited no osteolytic lesions.

The right leg of mice harboring JJN3 cells initially displayed mechanical allodynia (Figure 2A) and thermal hyperalgesia (Figure 2B) at day 20 of post injection and these pain behaviors progressed in parallel with bone destruction. Sham mice showed no evidence of MMBP (Figure 2A, 2B). Left legs of JJN3-injected mice had no evidence of MMBP, demonstrating that MMBP is associated with local JJN3 colonization rather than a systemic effect of JJN3 cells. Sprouting of $CGRP^+$ SNs in JJN3-injected bone was increased in parallel with the progression of MMBP (Figure 2C, 2D).

5TGM1 MM cells intratibilally injected into immunocompetent C57BL/KaLwRij mice also developed osteolytic lesions and induced progressive MMBP (Supplemental Figure 1A and 1B).

Acidification and MMBP are associated with JJN3-colonized bone

We next determined if the JJN3-colonized bone is acidic using the pH sensor fluorescent dye, acridine orange. No fluorescence was detected in the right tibiae of sham mice (Figure 2E, left). In contrast, the entire marrow of right tibiae injected with JJN3 cells was fluorescent (Figure 2E, center), demonstrating that JJN3-colonized bone is acidic. The bone marrow injected with 5TGM1 cells was also acidic (Supplemental Figure 1D, right). We then assessed if the selective V-ATPase inhibitor, bafilomycin A1 (Baf A1), blocked established MMBP in JJN3-injected mice. Baf A1 inhibited acidification by OCL bone resorption (40), and, we reported, reduced bone pain in BC bone metastases (41). Repeated injections of Baf A1 inhibited tumor growth (42) and bone resorption (40) that alter the status of bone pain. To examine if Baf A1 directly inhibits SN activation and reduces MMBP independent of inhibition of tumor growth and bone resorption, JJN3-injected mice manifesting MMBP and sham mice were given a single intraperitoneal injection of Baf A1 at day 25 (arrow in Figure 2A and 2B) and evaluated for changes in MMBP as a function of time. Baf A1 treatment blocked acidification in JJN3-colonized bone (Figure 2E, right). Importantly, Baf A1 blockade of the acidification of JJN3-colonized bone inhibited the progression of mechanical allodynia (Figure 2F) and thermal hyperalgesia (Figure 2G) as early as 12h after injection. The effects lasted up to 24h and were lost by 48h after injection.

In parallel with noxious behaviors, JJN3-injected mice demonstrated increased expression of pERK1/2 and pCREB, which are molecular indicators for neuronal excitation (43), in their DRG SNs compared with sham mice (Figure 2H). Similarly, 5TGM1-injected mice also exhibited elevated expression of pERK and pCREB in their DRG SNs (Supplemental Figure 1C). Importantly, the elevated levels of pERK1/2 and pCREB in DRG SNs in JJN3-injected mice were decreased at 12h after Baf A1 injection (Figure 2H), indicating that SN excitation, as well as noxious behaviors, is inhibited by blocking the acidification of JJN3-

colonized bone. These results suggest that H^+ released via V-ATPase directly excite SNs in bone to evoke MMBP. They also suggest that Baf A1 ameliorates MMBP by inhibiting SN excitation in a time period too short to be due to inhibition of JJN3 tumor growth and bone resorption.

Expression of V-ATPase and pH_e in JJN3 cells

We next examined if JJN3 cells contribute to acidification of the bone microenvironment by releasing H^+ via V-ATPase. Human MM cell lines, JJN3, H929 and U266, and MDA-MB-231 human BC cell line (serve as a positive control) expressed a3V-ATPase (Figure 3A). Importantly, $CD138^+$, but not $CD138^-$, cells derived from three MM patients expressed a3V-ATPase (Figure 3B). JJN3 expressed the a3V-ATPase on their plasma membrane (Figure 3C), as did highly-invasive MDA-MB-231 cells (44). The pH_e of JJN3, H929 and U266 and MDA-MB-231 and $CD138^+$ cells was acidic (Figure 3D). The human MM cells MM.1S expressed undetectable a3V-ATPase (Figure 3A) and the pH_e of MM.1S was not acidic (Figure 3D). The expression of a3V-ATPase in MC3T3-E1 osteoblastic and MLO-A5 and MLO-Y4 osteocytic cells was undetectable (Figure 3A) and their pH_e was not acidic (Figure 3D). Thus, osteoblasts and osteocytes unlikely contribute to extracellular acidification of MM-colonized bone. Baf A1 significantly blocked extracellular acidification in JJN3 cultures (Figure 3E) with no inhibition of cell proliferation (Figure 3F). In contrast, Baf A1 showed no effects on pH_e in other cells. Further, knockdown of a3V-ATPase in JJN3 cells significantly blocked extracellular acidification (Figure 3G).

Thus, the a3V-ATPase contributes to the acidification of JJN3 cell extracellular microenvironment. 5TGM1 cells also expressed plasma membrane a3V-ATPase and the pH_e of 5TGM1 cells was acidic, which was neutralized by Baf A1 (Supplementary Figure 1E-1G).

Effects of acidic microenvironment of JJN3-colonized bone on SNs

Tumors in bone induce SN sprouting in bone, thereby enhancing bone pain (13,14). We therefore determined the extent of $CGRP^+$ SN sprouting with or without treatment with Baf A1 in JJN3-colonized bone. Baf A1 inhibited the progression of mechanical allodynia in mice injected intratibially with JJN3 cells (Figure 4A). IHC showed increased $CGRP^+$ SN sprouting within the $CD138^+$ JJN3 tumor in tibiae (Figure 4B, middle and 4C) compared to tibiae of sham mice (Figure 4B, top and 4C). Treatment with Baf A1 decreased the sprouting of $CGRP^+$ SNs within the JJN3 tumor in bone (Figure 4B, bottom and 4C).

Thus, the acidic microenvironment of JJN3-colonized bone resulting from H^+ release via V-ATPase increases sprouting of $CGRP^+$ SNs *in vivo*.

To further analyze the effects of the acidic microenvironment created by JJN3 cells on SN sprouting, 1° N cells were co-cultured with JJN3 cells and assessed for neurite outgrowth, an *in vitro* indicator for sprouting (45). Neurite outgrowth of 1°N cells was increased in the co-cultures (Figure 4D and 4E). Importantly, Baf A1 significantly decreased neurite outgrowth of primary DRG neuron cells in the co-cultures (Figure 4D and 4E). Further, neurite outgrowth of 1°N cells cultured in media at pH 6.5, which is equivalent to the pH_e of JJN3 cultures, was also increased compared to that cultured in media at pH 7.4 (Figure 4F).

Thus, H^+ released via V-ATPase from JJN3 cells increase neurite outgrowth of SNs *in vitro*.

Activation of acid-sensing nociceptors by the acidic microenvironment of JJN3-colonized bone

To study the mechanism underlying increased sprouting of $CGRP^+$ SNs in bone occurring in the acidic microenvironment of JJN3 cells, we determined the expression of the acid-sensing nociceptors, ASIC3, on $CGRP^+$ SNs in DRG of JJN3-injected mice. We found increased expression of ASIC3 on $CGRP^+$ SNs of DRG in JJN3-injected mice by double immunofluorescent (Figure 5A) and Western analysis (Figure 5B) compared to sham mice. Expression of the acid-sensing nociceptor, TRPV1, was also increased on $CGRP^+$ SNs of DRG in JJN3-injected mice compared to sham mice (Supplemental Figure 2A and 2B). Increased neurite outgrowth of 1°N cells in co-cultures with JJN3 cells was reduced by treatment with the specific ASIC3 antagonist, APETx2 (46) or Baf A1 (Figure 5C).

We then examined the role of ASIC3 in SN excitation in response to JJN3-induced acidic microenvironment by assessing intracellular Ca^{2+} influx, an early indicator of SN excitation *in vitro* (38), in 1°N cells. Co-culture of 1°N cells with JJN3 cells rapidly induced a transient Ca^{2+} influx (Figure 5D, iii), which was blocked by APETx2 (Figure 5D, iv). Addition of culture medium caused no Ca^{2+} influx (Figure 5D, i). Addition of HCl at a final pH 6.5 also induced a Ca^{2+} influx (Figure 5E), while PBS at pH7.4 had no effect. Importantly, no Ca^{2+} influx was induced by the addition of JJN3 cells (Figure 5D, iv) or pH 6.5 medium (Figure 5F) when 1°N cells were pre-treated with APETx2 for 2h.

Thus, the acidic extracellular microenvironment of JJN3 cells promotes neurite outgrowth and excites 1°N SNs via ASIC3 activation.

Role of ASIC3 in MMBP

We then determined the role of ASIC3 in MMBP by testing APETx2 *in vivo*. JJN3-bearing and sham mice were treated with a single intraplantar injection of APETx2 at day 25 (arrow in Figure 6A) and evaluated for changes in MMBP. APETx2 reduced mechanical allodynia as early as 1h after injection, which lasted until 12h and disappeared after 24h (Figure 6B, open square). As shown in Figure 2G, Baf A1 exhibited its analgesic effects 12h after injection until 24h (Figure 6B, open triangle) following a single intraperitoneal injection (arrow in Figure 6A).

Further, pERK1/2 and pCREB expression in DRG was decreased in APETx2- and Baf A1-treated JJN3-injected mice compared to vehicle-treated JJN3-injected mice at 6h after APETx2 injection (Figure 6C).

Thus, inhibition of ASIC3 or V-ATPase by APETx2 or Baf A1 administered in an “as-needed manner” alleviates MMBP, respectively. These results indicate that ASIC3 plays an important role in MMBP induced by acidic bone microenvironment.

The selective TRPV1 antagonist, SB366791, also alleviated mechanical allodynia and decreased pERK1/2 and pCREB in DRG in JJN3-injected mice following a single intraplantar injection (Supplemental Figure 2C and 2D).

Effects of inhibition of both V-ATPase and ASIC3 on SNs on MMBP

The analgesic effects of APETx2 were observed 1h after injection and lost after 18h (Figure 6B, open square), whereas Baf A1 exhibited its analgesic effects 12h after injection until 24h (Figure 6B, open triangle). We therefore examined if treatment of JJN3-injected mice with a combination of APETx2 and Baf A1 produces rapid and sustained analgesic effects on MMBP. As expected, combined treatment with a single intraplantar injection of APETx2 and a single intraperitoneal injection of Baf A1 decreased mechanical allodynia (Figure 6B, closed square) as early as 1h after injection to a greater extent and for a longer period than did each agent alone.

Expression of pERK1/2 and pCREB in DRG in JJN3-injected mice was also more profoundly down-regulated by the combined treatment than each agent alone (Figure 6C).

Contributions of OCLs to MMBP

OCLs express a3V-ATPase on their plasma membrane in the ruffled border (15,47) through which H^+ are secreted during bone resorption, creating an acidic extracellular microenvironment (15–17). Histological examination of bone of JJN3-injected mice showed that the pits formed by $TRAP^+$ OCLs on endosteal bone surfaces (Figure 7A, top) were acidic (Figure 7A, bottom, arrowheads), and that $CGRP^+$ SNs innervated in close proximity to $TRAP^+$ OCLs (Figure 7B). These findings suggest that the OCL-generated acidic microenvironments can directly activate pH-sensitive SNs in bone and elicit MMBP. To determine the role of OCLs in SN activation and MMBP, we tested the potent inhibitor of OCLs, zoledronic acid (ZOL), which reduces MMBP in patients (2). JJN3-injected mice (Figure 7C, closed circle) were treated with ZOL at day 10, 14 and 18 (arrows in 7C) using an established protocol (48). ZOL significantly reduced mechanical allodynia (Figure 7C, closed triangle). Of note, however, the analgesic effects of ZOL were lost at day 35. These results are consistent with the clinical observations that ZOL does not prevent the progression of bone pain in MM patients at advanced stages (2,3,22), and suggest that suppression of OCL bone resorption no longer ameliorates MMBP and that MM cells predominantly contribute to MMBP at advanced stages.

Effects of inhibition of both OCLs and V-ATPase on MMBP

We therefore examined if inhibition of H^+ release via V-ATPase from JJN3 cells by Baf A1 alleviates MMBP that became refractory to analgesic effects of ZOL. As already shown in Figure 2G and Figure 6B, a single intraperitoneal injection of Baf A1 to untreated JJN3-bearing mice reduced MMBP (Figure 7D, closed diamond). Of note, a single intraperitoneal injection of Baf A1 to ZOL-treated JJN3-bearing mice that lost responsiveness to analgesic effects of ZOL at day 35 (arrowhead in 7C) decreased mechanical allodynia (Figure 7D, closed square) as early as 1h until 24h. Further, the combination of Baf A1 and ZOL decreased pERK1/2 and pCREB expression in DRG more profoundly than did ZOL or Baf A1 alone (Figure 7E). These results indicate that V-ATPase on MM cells as well as OCLs contribute to SN excitation and MMBP at advanced stages of MM.

Discussion

We investigated the contributions of the acidic bone microenvironment associated with MM colonization in bone to MMBP. We showed that bone-colonizing JJN3 cells release H^+ via V-ATPase, creating an acidic bone microenvironment. This pathological acidic microenvironment then stimulates the sprouting of $CGRP^+$ SNs innervating bone and activates the acid-sensing nociceptors, ASIC3, on the $CGRP^+$ SNs, which in turn excites the SNs to evoke MMBP. Blocking H^+ release and development of the acidic bone microenvironment by the selective V-ATPase inhibitor, Baf A1, decreased the sprouting of $CGRP^+$ SNs in bone, inhibited the excitation of the SNs and reduced MMBP in JJN3-injected mice. Inhibiting H^+-induced activation of ASIC3 by the specific ASIC3 antagonist, APETx2, inhibited SN excitation and alleviated MMBP. Further, a combination of a single injection of Baf A1 and APETx2 showed greater and longer analgesic effects on MMBP than each agent alone. Taken together, these results indicate that secretion of H^+ via V-ATPase on MM cells and subsequent activation of SNs by H^+ via ASCI3 are key steps responsible for inducing MMBP and that these steps could be mechanism-based targets for treatment of MMBP in patients.

Our results for the first time show that not only OCLs but also MM cells directly contribute to SN activation to evoke MMBP through releasing H^+ via V-ATPase. The result in part explains the observations that OCL-specific inhibitors alone reduce MMBP at early to advanced stages, however, fail to prevent the progression of MMBP at advanced to terminal stages of the disease (2,20). Consistent with these observations, ZOL reduced MMBP at early stages but lost its analgesic effects at terminal stages in our animal model. Of importance, amelioration of MMBP was restored by additional administration of a single injection of Baf A1 to ZOL-treated mice, demonstrating that blockade of H^+ release from MM cells via suppression of V-ATPase mitigates MMBP refractory to the analgesic action of ZOL. These results suggest that administration of V-ATPase inhibitor combined with OCL inhibitor may be an effective approach for management of MMBP in patients with advanced MM.

ZOL was shown to decrease tumor burden in preclinical models of MM (48). Thus, alleviation of MMBP by ZOL in JJN3-injected mice could be secondary to decreased MM tumor burden rather than inhibition of OCL bone resorption. However, clinical observations that ZOL fails to prevent the progression of MMBP at advanced stages of the disease (2,20) together with our results suggest that the analgesic effects of ZOL are unlikely accounted by inhibition of MM growth.

Expression of the acid-sensing nociceptor TRPV1 was also increased on $CGRP^+$ SNs in JJN3-injected mice. Previous studies reported that TRPV1 antagonists or disruption of the TRPV1 gene attenuated cancer-induced bone pain (28,29). We also showed that a single intraplantar injection of the selective TRPV1 antagonist, SB366791, significantly decreased SN excitation and MMBP in JJN3-injected mice. TRPV1 on SNs is activated at $pH < 6.0$ (27). The pH_e of the acidic microenvironment created by JJN3 cells and bone-resorbing OCLs is 6.5–6.9 (Figure 3) and 4.5–6.0 (15–17), respectively. These results suggest that the pH_e of specific areas in JJN3-colonized bone may be < 6.0, a pH at which TRPV1 is

activated. We propose that the pH_e of MM-colonized bone varies spatially and temporally, and induces activation of either ASIC3, TRPV1 or both on pH-sensitive SNs to induce MMBP, depending on the status of MM progression and OCL bone resorption.

Although our results demonstrate significant contribution of bone-resorbing OCL to MMBP in JJN3-injected mice, OCL bone resorption that occurs under physiological conditions rarely induces bone pain. As an explanation for this, recent studies reported that TRPV1 and ASIC3 dramatically decrease their threshold for sensing noxious stimuli in the presence of tissue damage and inflammation (18). Thus, it is speculated that SNs are not sensitive enough to be excited to evoke bone pain in response to acidic microenvironments created by physiological OCL bone resorption. Further, episodic musculoskeletal pain termed “growing pain” that often occurs in children in early childhood (49) suggests that bone turnover rate may be critical.

Solid tumors express various plasma membrane pH-regulators, including V-ATPase, monocarboxylate transporter 1/4, and carbonic anhydrases (24) through which H^+ are extruded to avoid intracellular acidification due to elevated aerobic glycolysis (Warburg effect) (50), and acidify the extracellular microenvironment. Among these pH-regulators, a3V-ATPase has been implicated in solid cancer invasiveness and metastasis (25,44). We previously reported that suppression of a3V-ATPase in highly-metastatic B16-F10 melanoma decreases bone metastasis (51). In contrast, if MM cells express V-ATPase was unknown. Here we show that JJN3 cells express plasma membrane a3V-ATPase that acidifies extracellular environments by releasing H^+ and directly contributes to SN activation to induce MMBP. However, whether a3V-ATPase expression is associated with MM progression as is the case of solid tumors is unknown. Our results showed that a single injection of Baf A1 had no effects on JJN3 progression in bone and that Baf A1 did not inhibit JJN3 proliferation in culture, although long-term effects of Baf A1 on MM progression were not examined in this study. Interestingly, however, $CD138^+$ primary cells derived from bone marrow of MM patients expressed a3V-ATPase, while little expression of a3V-ATPase was seen in $CD138^-$ cells. Further studies are needed to determine the relationship between a3V-ATPase expression and MM progression.

In conclusion, this study shows that the creation of acidic extracellular bone microenvironments by OCLs and MM cells via H^+ secretion through plasma membrane V-ATPase and responses of SNs innervating bone to the acidic microenvironment via ASIC3 are critical contributors to the pathophysiology of MMBP. Targeting these pathways may provide mechanism-based effective therapies for control of MMBP, which is currently under-treated.

Supplementary Material

Refer to Web version on PubMed Central for supplementary material.

Acknowledgments

This study was supported by the Project Development Team within the ICTSI NIH/NCRR (#TR000006), the Indiana University Health Strategic Research Initiative in Oncology, and start-up fund of Indiana University School

of Medicine (to T. Yoneda) and Merit Review Funds from the Veterans Administration (to G.D. Roodman), the NIH (#DK100905; to F.A.White), and MERIT Review Award (#BX002209) from the U.S. Department of Veterans Affairs, Biomedical Laboratory Research and Development Service (to F.A. White). Support for Y.M. Allette as an Indiana CTSI Predoctoral trainee was provided by UL1 (#TR001108), NIH/NCATS (A. Shekhar, principal investigator), and Japan Society for the Promotion of Science Grants-in-aid for Research Activity Start-up, and Postdoctoral Fellowship for Research Abroad (to M. Hiasa).

References

1. Kyle RA, Rajkumar SV. Multiple myeloma. Blood. 2008; 111:2962–2972. [PubMed: 18332230]
2. Terpos E, Berenson J, Raje N, Roodman GD. Management of bone disease in multiple myeloma. Expert Rev Hematol. 2014; 7:113–125. [PubMed: 24433088]
3. Niscola P, Scaramucci L, Romani C, Giovannini M, Tendas A, Brunetti G, et al. Pain management in multiple myeloma. Expert Rev Anticancer Ther. 2010; 10:415–425. [PubMed: 20214522]
4. Ganz PA, Coscarelli A, Fred C, Kahn B, Polinsky ML, Petersen L. Breast cancer survivors: psychosocial concerns and quality of life. Breast Cancer Res Treat. 1996; 38:183–199. [PubMed: 8861837]
5. Burrows M, Dibble SL, Miaskowski C. Differences in outcomes among patients experiencing different types of cancer-related pain. Oncol Nurs Forum. 1998; 25:735–741. [PubMed: 9599356]
6. Poulos AR, Gertz MA, Pankratz VS, Post-White J. Pain, mood disturbance, and quality of life in patients with multiple myeloma. Oncol Nurs Forum. 2001; 28:1163–1171. [PubMed: 11517849]
7. Whitelaw DM. Pain in multiple myeloma. Can Med Assoc J. 1963; 88:1242–1243. [PubMed: 14000379]
8. Cooper RR. Nerves in cortical bone. Science. 1968; 160:327–328. [PubMed: 5641266]
9. Irie K, Hara-Irie F, Ozawa H, Yajima T. Calcitonin gene-related peptide (CGRP)-containing nerve fibers in bone tissue and their involvement in bone remodeling. Microsc Res Tech. 2002; 58:85–90. [PubMed: 12203707]
10. Mach DB, Rogers SD, Sabino MC, Luger NM, Schwei MJ, Pomonis JD, et al. Origins of skeletal pain: sensory and sympathetic innervation of the mouse femur. Neuroscience. 2002; 113:155–166. [PubMed: 12123694]
11. Mantyh P. Bone cancer pain: causes, consequences, and therapeutic opportunities. Pain. 2013; (154 Suppl 1):S54–S62. [PubMed: 23916671]
12. Fukuda T, Takeda S, Xu R, Ochi H, Sunamura S, Sato T, et al. Sema3A regulates bone-mass accrual through sensory innervations. Nature. 2013; 497:490–493. [PubMed: 23644455]
13. Mantyh WG, Jimenez-Andrade JM, Stake JI, Bloom AP, Kaczmarska MJ, Taylor RN, et al. Blockade of nerve sprouting and neuroma formation markedly attenuates the development of late stage cancer pain. Neuroscience. 2010; 171:588–598. [PubMed: 20851743]
14. Jimenez-Andrade JM, Bloom AP, Stake JI, Mantyh WG, Taylor RN, Freeman KT, et al. Pathological sprouting of adult nociceptors in chronic prostate cancer-induced bone pain. J Neurosci. 2010; 30:14649–14656. [PubMed: 21048122]
15. Qin A, Cheng TS, Pavlos NJ, Lin Z, Dai KR, Zheng MH. V-ATPases in osteoclasts: structure, function and potential inhibitors of bone resorption. Int J Biochem Cell Biol. 2012; 44:1422–1435. [PubMed: 22652318]
16. Kikuta J, Wada Y, Kowada T, Wang Z, Sun-Wada GH, Nishiyama I, et al. Dynamic visualization of RANKL and Th17-mediated osteoclast function. J Clin Invest. 2013; 123:866–873. [PubMed: 23321670]
17. Sano H, Kikuta J, Furuya M, Kondo N, Endo N, Ishii M. Intravital bone imaging by two-photon excitation microscopy to identify osteocytic osteolysis in vivo. Bone. 2015; 74:134–139. [PubMed: 25624000]
18. Basbaum AI, Bautista DM, Scherrer G, Julius D. Cellular and molecular mechanisms of pain. Cell. 2009; 139:267–284. [PubMed: 19837031]
19. Mantyh PW. Cancer pain and its impact on diagnosis, survival and quality of life. Nat Rev Neurosci. 2006; 7:797–809. [PubMed: 16988655]

20. Terpos E, Morgan G, Dimopoulos MA, Drake MT, Lentzsch S, Raje N, et al. International Myeloma Working Group recommendations for the treatment of multiple myeloma-related bone disease. J Clin Oncol. 2013; 31:2347–2357. [PubMed: 23690408]
21. Kohno N, Aogi K, Minami H, Nakamura S, Asaga T, Iino Y, et al. Zoledronic acid significantly reduces skeletal complications compared with placebo in Japanese women with bone metastases from breast cancer: a randomized, placebo-controlled trial. J Clin Oncol. 2005; 23:3314–3321. [PubMed: 15738536]
22. Cleeland CS, Body JJ, Stopeck A, von Moos R, Fallowfield L, Mathias SD, et al. Pain outcomes in patients with advanced breast cancer and bone metastases: results from a randomized, double-blind study of denosumab and zoledronic acid. Cancer. 2013; 119:832–838. [PubMed: 22951813]
23. von Moos R, Body JJ, Egerdie B, Stopeck A, Brown JE, Damyanov D, et al. Pain and health-related quality of life in patients with advanced solid tumours and bone metastases: integrated results from three randomized, double-blind studies of denosumab and zoledronic acid. Support Care Cancer. 2013; 21:3497–3507. [PubMed: 23975226]
24. Neri D, Supuran CT. Interfering with pH regulation in tumours as a therapeutic strategy. Nat Rev Drug Discov. 2011; 10:767–777. [PubMed: 21921921]
25. Gatenby RA, Gawlinski ET, Gmitro AF, Kaylor B, Gillies RJ. Acid-mediated tumor invasion: a multidisciplinary study. Cancer Res. 2006; 66:5216–5223. [PubMed: 16707446]
26. Krames ES. The dorsal root ganglion in chronic pain and as a target for neuromodulation: a review. Neuromodulation. 2015; 18:24–32. discussion. [PubMed: 25354206]
27. Caterina MJ, Leffler A, Malmberg AB, Martin WJ, Trafton J, Petersen-Zeitz KR, et al. Impaired nociception and pain sensation in mice lacking the capsaicin receptor. Science. 2000; 288:306–313. [PubMed: 10764638]
28. Ghilardi JR, Rohrich H, Lindsay TH, Sevcik MA, Schwei MJ, Kubota K, et al. Selective blockade of the capsaicin receptor TRPV1 attenuates bone cancer pain. J Neurosci. 2005; 25:3126–3131. [PubMed: 15788769]
29. Niiyama Y, Kawamata T, Yamamoto J, Furuse S, Namiki A. SB366791, a TRPV1 antagonist, potentiates analgesic effects of systemic morphine in a murine model of bone cancer pain. Br J Anaesth. 2009; 102:251–258. [PubMed: 19038965]
30. Deval E, Noel J, Lay N, Alloui A, Diochot S, Friend V, et al. ASIC3, a sensor of acidic and primary inflammatory pain. Embo j. 2008; 27:3047–3055. [PubMed: 18923424]
31. Storti P, Bolzoni M, Donofrio G, Airoldi I, Guasco D, Toscani D, et al. Hypoxia-inducible factor (HIF)-1alpha suppression in myeloma cells blocks tumoral growth in vivo inhibiting angiogenesis and bone destruction. Leukemia. 2013; 27:1697–1706. [PubMed: 23344526]
32. Hiasa M, Teramachi J, Oda A, Amachi R, Harada T, Nakamura S, et al. Pim-2 kinase is an important target of treatment for tumor progression and bone loss in myeloma. 2015; 29:207–217.
33. Ugolini G, Marinelli S, Covaceuszach S, Cattaneo A, Pavone F. The function neutralizing anti-TrkA antibody MNAC13 reduces inflammatory and neuropathic pain. Proc Natl Acad Sci U S A. 2007; 104:2985–2990. [PubMed: 17301229]
34. Ramer LM, Borisoff JF, Ramer MS. Rho-kinase inhibition enhances axonal plasticity and attenuates cold hyperalgesia after dorsal rhizotomy. J Neurosci. 2004; 24:10796–10805. [PubMed: 15574730]
35. Currie GL, Delaney A, Bennett MI, Dickenson AH, Egan KJ, Vesterinen HM, et al. Animal models of bone cancer pain: systematic review and meta-analyses. Pain. 2013; 154:917–926. [PubMed: 23582155]
36. Satonaka H, Kusuzaki K, Matsubara T, Shintani K, Wakabayashi T, Matsumine A, et al. Extracorporeal photodynamic image detection of mouse osteosarcoma in soft tissues utilizing fluorovisualization effect of acridine orange. Oncology. 2006; 70:465–473. [PubMed: 17237622]
37. Meijering E, Jacob M, Sarria JC, Steiner P, Hirling H, Unser M. Design and validation of a tool for neurite tracing and analysis in fluorescence microscopy images. Cytometry A. 2004; 58:167–176. [PubMed: 15057970]
38. Due MR, Park J, Zheng L, Walls M, Allette YM, White FA, et al. Acrolein involvement in sensory and behavioral hypersensitivity following spinal cord injury in the rat. J Neurochem. 2014; 128:776–786. [PubMed: 24147766]

39. Sun-Wada GH, Tabata H, Kuhara M, Kitahara I, Takashima Y, Wada Y. Generation of chicken monoclonal antibodies against the a1, a2, and a3 subunit isoforms of vacuolar-type proton ATPase. Hybridoma (Larchmt). 2011; 30:199–203. [PubMed: 21529295]
40. Henriksen K, Sorensen MG, Jensen VK, Dziegiel MH, Nosjean O, Karsdal MA. Ion transporters involved in acidification of the resorption lacuna in osteoclasts. Calcif Tissue Int. 2008; 83:230–242. [PubMed: 18787885]
41. Nagae M, Hiraga T, Yoneda T. Acidic microenvironment created by osteoclasts causes bone pain associated with tumor colonization. J Bone Miner Metab. 2007; 25:99–104. [PubMed: 17323179]
42. Xu J, Xie R, Liu X, Wen G, Jin H, Yu Z, et al. Expression and functional role of vacuolar H(+)-ATPase in human hepatocellular carcinoma. Carcinogenesis. 2012; 33:2432–2440. [PubMed: 22962303]
43. Kawasaki Y, Kohno T, Zhuang ZY, Brenner GJ, Wang H, Van Der Meer C, et al. Ionotropic and metabotropic receptors, protein kinase A, protein kinase C, and Src contribute to C-fiber-induced ERK activation and cAMP response element-binding protein phosphorylation in dorsal horn neurons, leading to central sensitization. J Neurosci. 2004; 24:8310–8321. [PubMed: 15385614]
44. Cotter K, Capecci J, Sennoune S, Huss M, Maier M, Martinez-Zaguilan R, et al. Activity of plasma membrane V-ATPases is critical for the invasion of MDA-MB231 breast cancer cells. J Biol Chem. 2015; 290:3680–3692. [PubMed: 25505184]
45. Meldolesi J. Neurite outgrowth: this process, first discovered by Santiago Ramon y Cajal, is sustained by the exocytosis of two distinct types of vesicles. Brain Res Rev. 2011; 66:246–255. [PubMed: 20600308]
46. Diochot S, Baron A, Rash LD, Deval E, Escoubas P, Scarzello S, et al. A new sea anemone peptide, APETx2, inhibits ASIC3, a major acid-sensitive channel in sensory neurons. Embo j. 2004; 23:1516–1525. [PubMed: 15044953]
47. Toyomura T, Murata Y, Yamamoto A, Oka T, Sun-Wada GH, Wada Y, et al. From lysosomes to the plasma membrane: localization of vacuolar-type H+ -ATPase with the a3 isoform during osteoclast differentiation. J Biol Chem. 2003; 278:22023–22030. [PubMed: 12672822]
48. Croucher PI, De Hendrik R, Perry MJ, Hijzen A, Shipman CM, Lippitt J, et al. Zoledronic acid treatment of 5T2MM-bearing mice inhibits the development of myeloma bone disease: evidence for decreased osteolysis, tumor burden and angiogenesis, and increased survival. J Bone Miner Res. 2003; 18:482–492. [PubMed: 12619933]
49. Uziel Y, Hashkes PJ. Growing pains in children. Pediatr Rheumatol Online J. 2007; 5:5. [PubMed: 17550631]
50. Vander Heiden MG, Cantley LC, Thompson CB. Understanding the Warburg effect: the metabolic requirements of cell proliferation. Science. 2009; 324:1029–1033. [PubMed: 19460998]
51. Nishisho T, Hata K, Nakanishi M, Morita Y, Sun-Wada GH, Wada Y, et al. The a3 isoform vacuolar type H(+)-ATPase promotes distant metastasis in the mouse B16 melanoma cells. Mol Cancer Res. 2011; 9:845–855. [PubMed: 21669964]

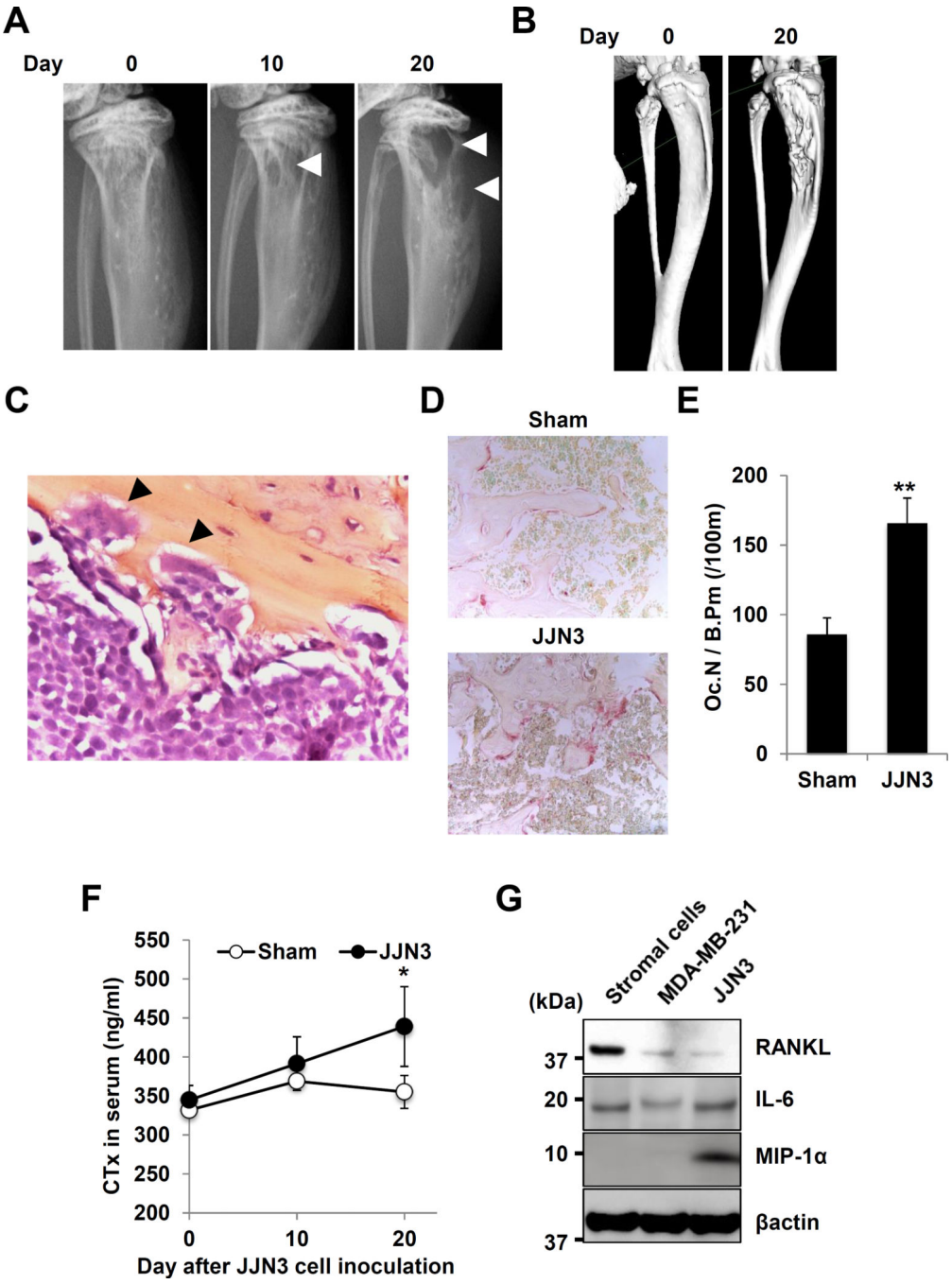

Figure 1. Development of osteolytic lesions in JJN3-injected mice

A. Radiographs of osteolytic lesions (arrowheads).

B. 3D μ-CT images.

C. JJN3 cells in bone marrow with OCL bone resorption (arrowheads, HE, x400).

D. TRAP staining of bone (x40).

E. Number of $TRAP^+$ OCL in bone. ** $p<0.01$ vs sham mice.

F. Serum CTx levels in mice. * $p<0.05$ vs sham mice.

G. Production of osteoclastogenic cytokines in JJN3 and MDA-MB-231 cells

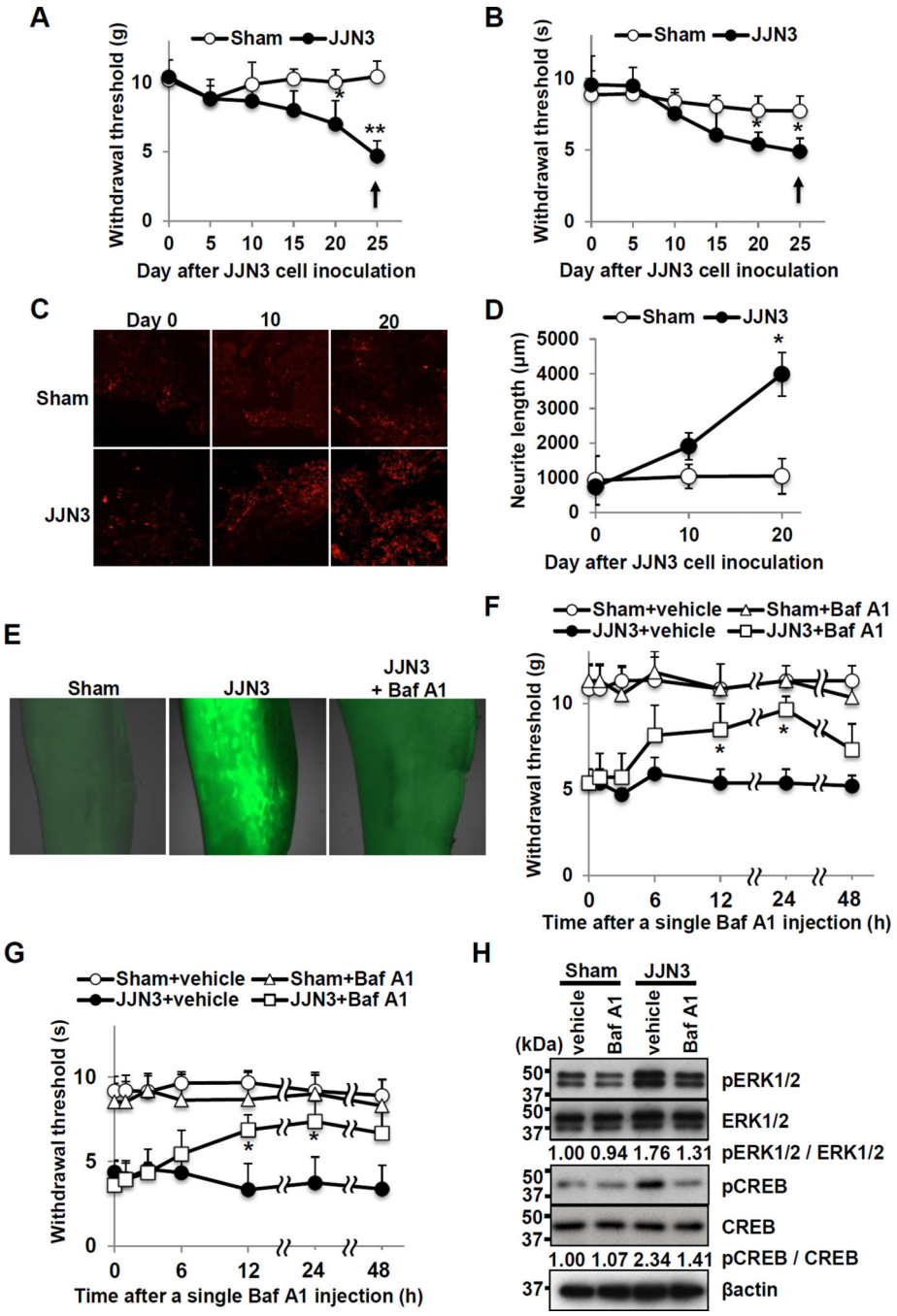

Figure 2. Bone pain and SN activation in JJN3-injected mice

A. Mechanical allodynia. * $p<0.05$, ** $p<0.01$ vs sham mice (mean ± SE, n=16). Arrow indicates a single intraperitoneal injection of Baf A1 (25μg/kg) or vehicle (0.1% DMSO in PBS).

B. Thermal hyperalgesia. * $p<0.05$ vs sham mice (mean ± SE, n=16). Arrow indicates a single intraperitoneal injection of Baf A1 (25μg/kg) or vehicle (0.1% DMSO in PBS).

C. Sprouting of $CGRP^+$ SNs in tibiae.

D. Quantitative data of C. * $p<0.05$ vs sham mice (mean ± SE, n=16).

E. Acidification of bone marrow shown by acridine orange accumulation.

F. Time-course of inhibition of mechanical allodynia, following a single intraperitoneal injection of Baf A1 (25μg/kg) or vehicle (0.1% DMSO in PBS) (arrow in A and B). * $p<0.05$ vs vehicle-treated JJN3-injected mice (mean ± SE, n=8).

G. Thermal hyperalgesia, following a single intraperitoneal injection of Baf A1 (25μg/kg) or vehicle (0.1% DMSO in PBS) (arrow in A and B). * $p<0.05$ vs vehicle-treated JJN3-injected mice (mean ± SE, n=8).

H. Excitation of sensory nerves determined by pERK1/2 and pCREB expression in DRG in sham and JJN3-injected mice.

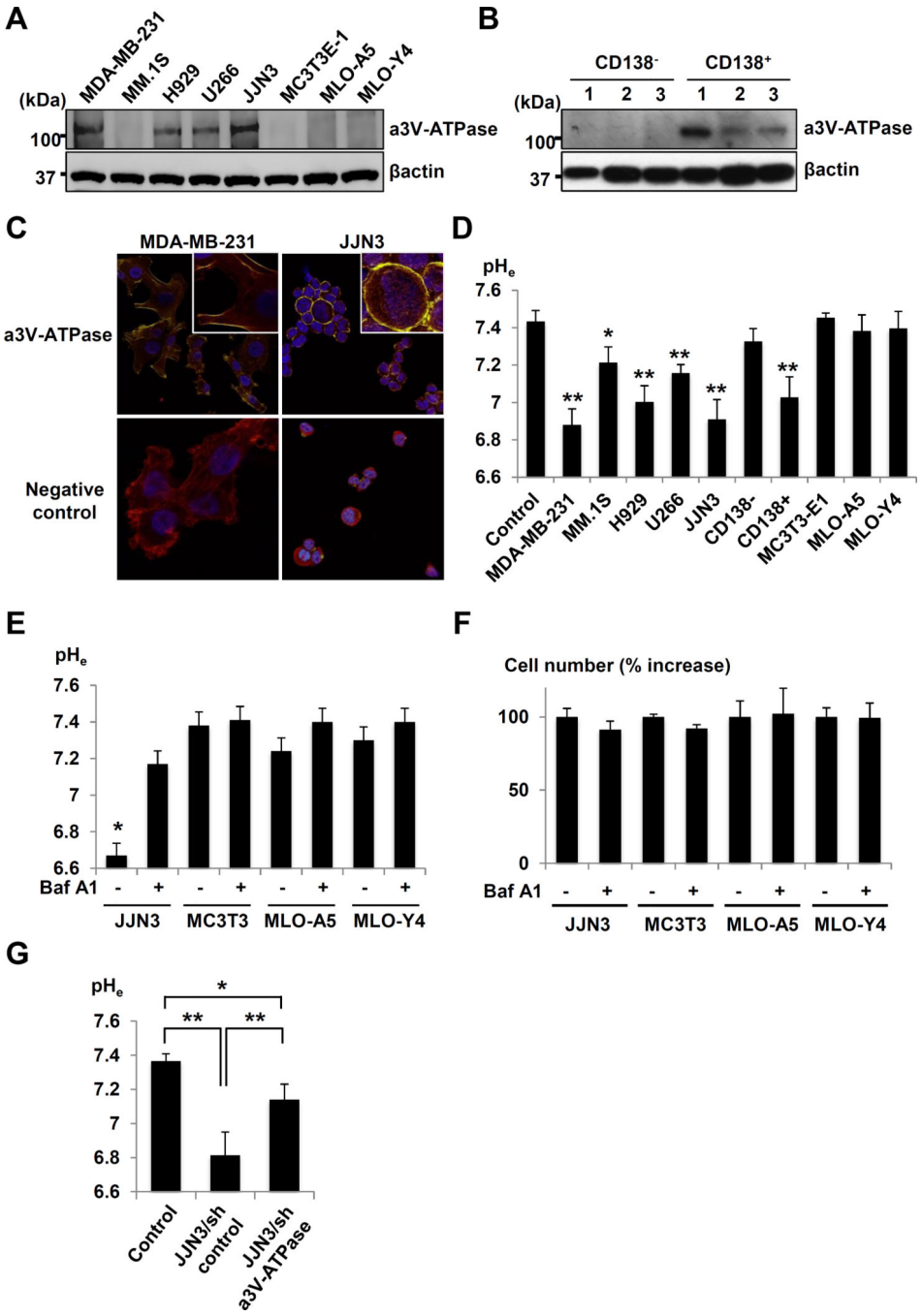

Figure 3. Expression of plasma membrane a3V-ATPase

A. a3V-ATPase expression in human MM cell lines (MM.1S, H929, U266 and JJN3), MC3T3-E1 mouse osteoblastic cells, MLO-A5 and MLO-Y4 mouse osteocytic cells, and MDA-MB-231 human breast cancer cells.

B. a3V-ATPase expression in primary $CD138^{+}$ and $CD138^{-}$ cells derived from three MM patients.

C. Immunocytochemsitry of a3V-ATPase expression in JJN3 and MDA-MB-231 cells.

D. pH_e in cultures of human MM cell lines, $CD138^+$ and $CD138^-$ cells, and MC3T3-E1, MLO-A5, MLO-Y4, and MDA-MB-231 cells. * $p<0.05$, ** $p<0.01$ vs control (mean ± SE, n=6).

E. Inhibition of acidification of pH_e by Baf A1 (50ng/ml, 48h). * $p<0.01$ vs Baf A1-treated JJN3 cells (mean ±SE, n=6).

F. Effects of Baf A1 (50ng/ml, 48h) on cell proliferation (mean ± SE, n=6).

G. pH_e in cultures of JJN3/sh a3V-ATPase or /sh control cells. * $p<0.01$ vs control. ** $p<0.05$ vs JJN3/sh control cells (mean ± SE, n=6).

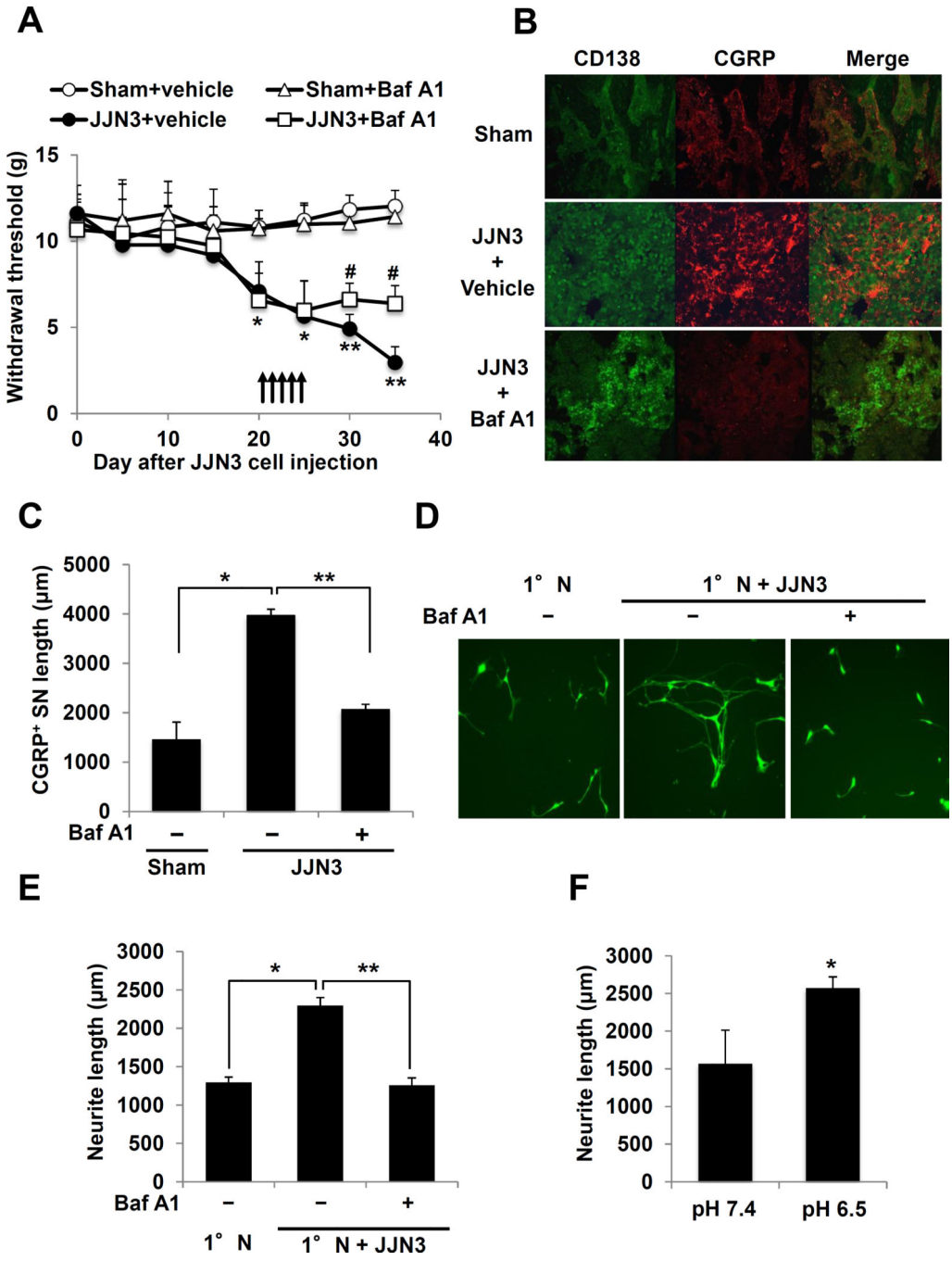

Figure 4. Sprouting and neurite outgrowth of SNs

A. Inhibition of mechanical allodynia by Baf A1 in JJN3-injected mice. Arrows: Baf A1 or vehicle injection. * $p<0.05$, ** $p<0.01$ vs sham mice. # $p<0.05$ vs vehicle-treated JJN3-injected mice (mean ± SE, n=8).

B. Sprouting of $CGRP^+$ SNs in tibiae. Left: CD138 (green); Center: CGRP (red); Right: merged image. Tibiae injected with, (top); PBS (sham), (middle); JJN3 cells and treated with vehicle, and (bottom); JJN3 cells and treated with Baf A1. Sections were incubated with

rabbit anti-CD138 (1:100) and goat anti-CGRP (1:200), then with donkey anti-rabbit IgG (1:100) and anti-goat IgG (1:100), respectively.

C. Quantitative analysis of B. * $p<0.01$ vs sham. ** $p<0.01$ vs vehicle-treated JJN3-injected tibiae (mean ± SE, n=6).

D. Neurite outgrowth from 1°N cells in co-culture with JJN3 cells. Co-cultures were treated with Baf A1 (50ng/ml) or vehicle (0.1% DMSO in PBS) for 5 days, labeled with calcein AM and quantitated.

E. Quantitative data of D. * $p<0.01$ vs 1°N cells alone. ** $p<0.01$ vs vehicle-treated co-cultures (mean ± SE, n=6).

F. Neurite outgrowth of 1°N cells. * $p<0.05$ vs pH 7.4 (mean ± SE, n=6).

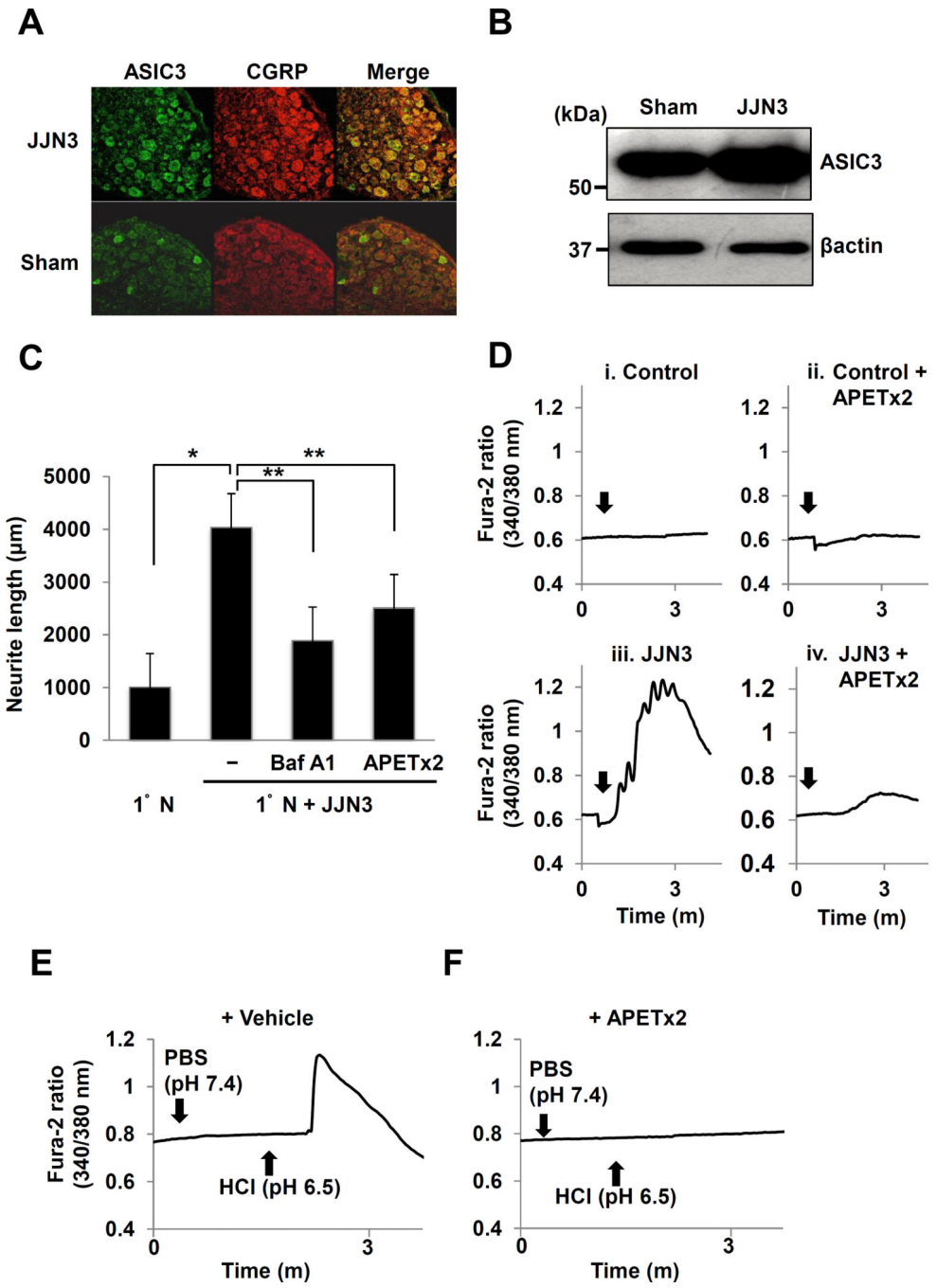

Figure 5. Role of ASIC3 in sprouting and excitation of SNs

A. Expression of ASIC3 (left, green) on CGRP^{+} SNs (center, red) in DRG from JJN3-injected (top) and sham mice (bottom). Sections were incubated with a goat anti-CGRP (1:200) and rabbit anti-ASIC3 (1:300), then a donkey anti-goat IgG (1:100) and anti-rabbit IgG (1:100), respectively.

B. ASIC3 expression in DRGs isolated from JJN3-injected and sham mice.

C. Neurite outgrowth from 1°N cells in co-cultures with JJN3 cells. Co-cultures were treated with Baf A1 (50ng/ml), APETx2 (0.5μM) or vehicle (0.1% DMSO in PBS) for 5 days. * $p<0.05$ vs 1°N cells alone. ** $p<0.05$ vs vehicle-treated co-cultures (mean ± SE, n=6).
D. Intracellular Ca^{2+} mobilization in co-cultures. 1°N cells were loaded with fura 2AM (3μM), treated with APETx2 (0.5μM) (ii and iv) or vehicle (0.1% DMSO in PBS) (i and iii) for 2h, then received JJN3 cells (3×10^5/300μl) (iii and iv) (arrows) or culture medium (i and ii), incubated and Ca^{2+} influx determined.
E. Ca^{2+} influx in 1°N cells. 1°N cells were pre-treated with APETx2 (0.5μM) for 2h, treated with PBS or HCl (arrows) and Ca^{2+} influx determined.

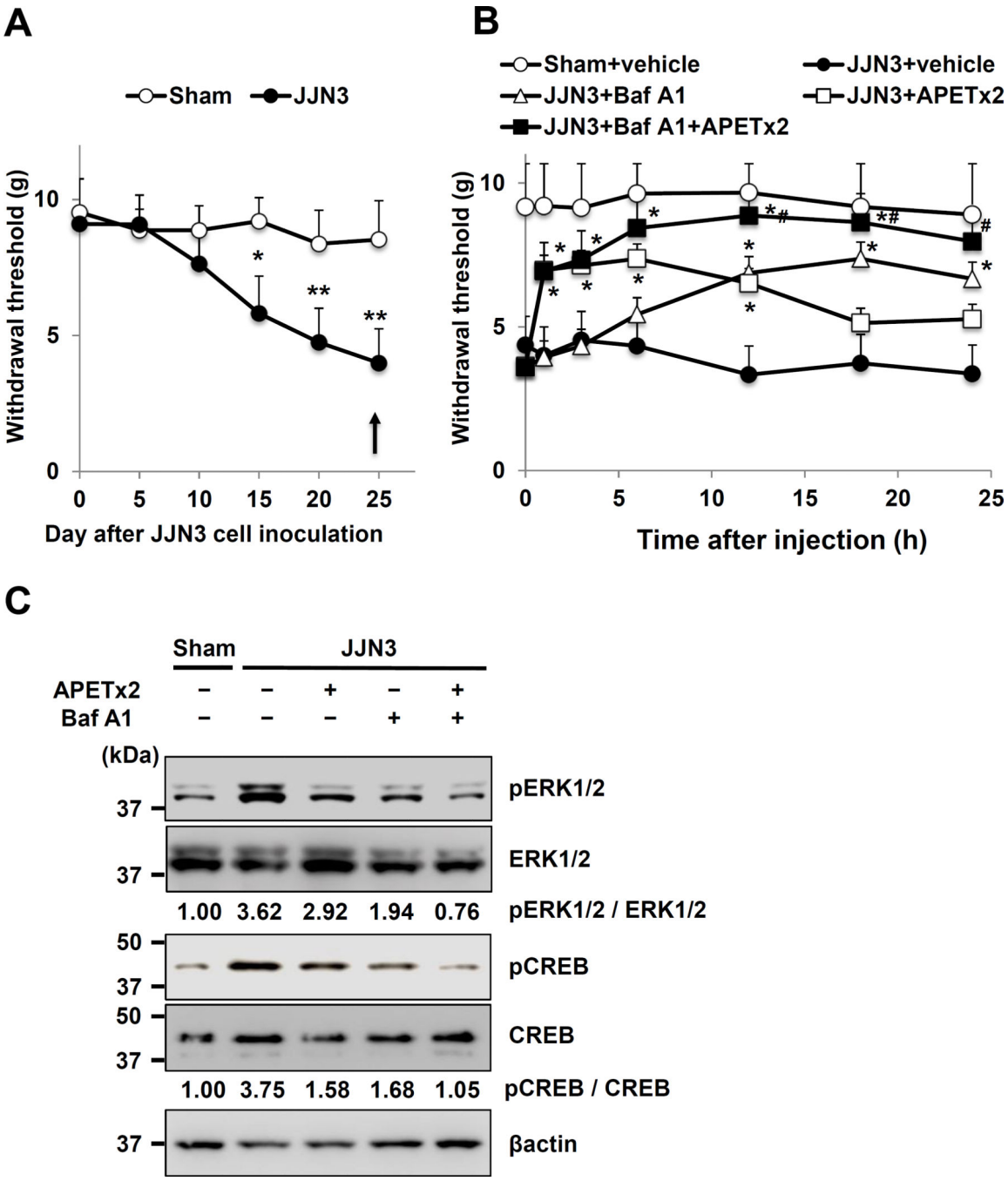

Figure 6. Contribution of a3V-ATPase and ASIC3 to MMBP and SN excitation

A. Mechanical allodynia. Arrow: a single injection of either vehicle, APETx2 (intraplantar), Baf A1 (intraperitoneal), or APETx2 combined with Baf A1. * $p<0.05$, ** $p<0.01$ vs sham (mean ± SE, n=8).

B. Time-course of inhibition of mechanical allodynia following treatment with either vehicle (0.1% DMSO in PBS), APETx2 (20μM), Baf A1 (25μg/kg) or APETx2 plus Baf A1 (arrow in A) in sham and JJN3-injected mice. * $p<0.05$ vs JJN3-injected mice treated with vehicle. # $p<0.05$ vs JJN3-injected mice treated with APETx2 or Baf A1 (mean ± SE, n=8).

C. Expression of pERK1/2 and pCREB in DRGs in mice shown in B at 12h.

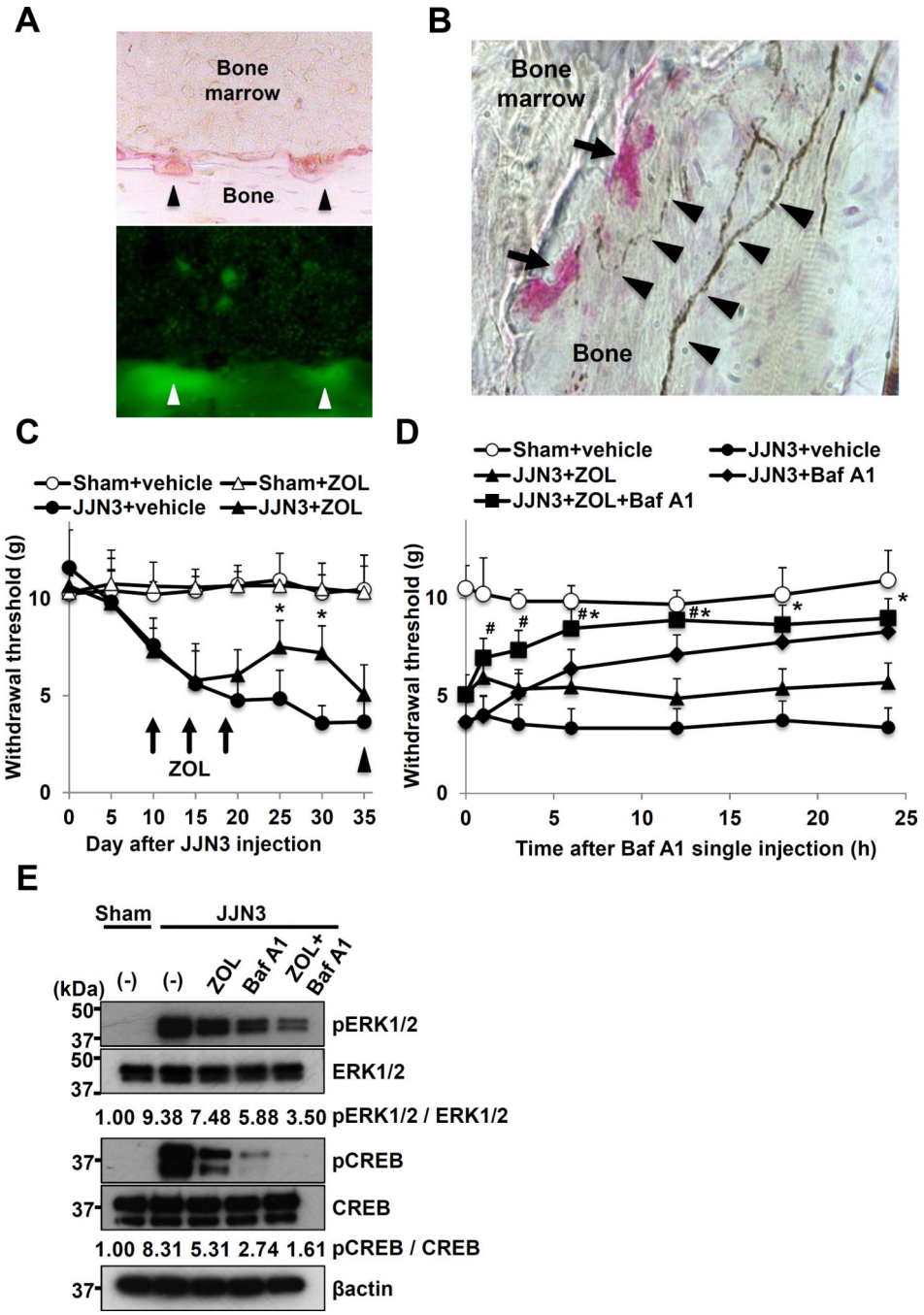

Figure 7. Contribution of OCL to MMBP and SN activation

A. Acidification of resorption lacunae formed on endosteal bone surfaces by TRAP$^+$ OCLs. Top: TRAP$^+$ OCLs (arrowheads) on endosteal bone surface. Bottom: Fluorescence of acridine orange accumulation in pits formed under OCLs (green). (x200)

B. Innervation of CGRP$^+$ SNs (arrowheads) in the close proximity of TRAP$^+$ OCLs (arrows). Sections were incubated with a goat anti-CGRP (1:200), followed by HRP-conjugated donkey anti-goat IgG (1:100). Brown: CGRP$^+$ SNs, Red: TRAP$^+$ OCLs. (x400)

C. Inhibition of mechanical allodynia by ZOL. Mice intratibially injected with JJN3 cells (●,▲) or PBS (sham) (○,△) were given vehicle (PBS) (○,●) or ZOL (120μg/kg) (△, ▲) at day 10, 14 and 18 after JJN3 cell injection (arrows). At day 35, mice were given a single intraperitoneal injection of Baf A1 (arrow head). * $p<0.05$ vs vehicle-treated, JJN3-injected mice (mean ± SE, n=8).

D. Effects of a single intraperitoneal injection of Baf A1 at day 35 (arrowhead in Figure 7C) on MMBP that became unresponsive to ZOL. At day 35, vehicle-treated JJN3-injected mice were given a single intraperitoneal injection of vehicle (●) or Baf A1 (◆), and ZOL-treated JJN3-injected mice received a single intraperitoneal injection of vehicle (▲) or Baf A1 (25μg/kg) (■). * $p<0.05$ vs ZOL-treated JJN3-injected mice. # $p<0.05$ vs Baf A1-treated JJN3-injected mice (mean ± SE, n=8).

E. Expression of pERK1/2 and pCREB in DRG SNs in mice shown in D at 12h.